

Bragg transmission phase plates for the production of circularly polarized x rays

J. C. Lang and George Srajer

Advanced Photon Source, Argonne National Laboratory, Argonne, Illinois 60439

(Presented 18 July 1994)

The x-ray optics for a thin-crystal Si (400) Bragg transmission phase plate have been constructed for the production of 5 to 12 keV circularly polarized x rays. Using multiple beam diffraction from a GaAs crystal, a direct measurement of the degree of circular polarization as a function of off-Bragg position was made. These measurements indicated nearly complete circular polarization ($|P_c| \geq 0.95$) and full helicity reversal on opposite sides of the rocking curve. © 1995 American Institute of Physics.

I. INTRODUCTION

The importance of photon helicity in spin-dependent magnetic interactions has led to a great deal of effort in obtaining high-quality circularly polarized x-ray (CPX) sources. Circularly polarized photons have definite angular momentum and thus couple with the moment of an atom allowing them to be used to probe the magnetic properties of materials. While this coupling has long been observed in the visible light region, it has only been recently demonstrated in the x-ray region, with the observation of magnetic Compton¹ and Bragg scattering,² and circular magnetic x-ray dichroism (CMXD).³ These polarization-modulated x-ray spectroscopy and diffraction experiments have shown great promise to provide unique information about the magnetic properties of condensed matter, but their development has been hampered by the lack of efficient CPX sources.

To be able to perform all these types of experiments, a CPX source ought to possess a few basic properties. First, since the magnetic cross section is much smaller than the Thomson cross section, the source should provide the highest possible photon flux and circular polarization rate (P_c) incident on the sample. Second, the source should be inherently stable, because these measurements generally involve differences in two spectra on the order of 0.1% and thus are very sensitive to energy shifts and changes in the polarization. Third, the source should be energy tunable, that is, able to achieve maximum circular polarization for any given energy. Finally, the source should accommodate frequent and rapid reversal of the photon helicity in order to avoid systematic errors arising from drift in the experimental apparatus. This ability to reverse the photon helicity is also essential in extending these types of measurements to hard magnetic materials and low temperatures where rapid reversal of the sample magnetization direction might not be possible.

While current CPX sources are able to provide some of these qualities, no one source has been able to combine them all. In this study, the optics for a thin-crystal Si (400) Bragg transmission phase plate have been constructed and tested. Measurements of the full polarization state of the transmitted beam indicate that this CPX source possesses all the desired qualities above. Therefore, this type of phase plate provides an energy tunable high P_c x-ray source which can rapidly change between photon helicities with minimal attenuation

of the x-ray beam, making it uniquely suited for magnetic x-ray scattering and absorption measurements.

II. BRAGG TRANSMISSION PHASE PLATE

Phase plates employ perfect crystal optics to transform linear to circular polarization by inducing a $\pm \pi/2$ phase shift between equal amounts of incoming σ and π polarized radiation. Being the final optical element before the experiment, they offer the greatest degree of circular polarization incident on the sample ($P_c \geq 0.9$). Furthermore, when utilized with an on-axis undulator beam, the amount of CPX flux delivered by phase plates can be comparable to that of a specialized insertion device but at a fraction of the cost. Three types of phase plates have been proposed and investigated up to now: (i) Bragg reflection,⁴ (ii) Laue reflection,¹ and (iii) Bragg transmission.⁵⁻⁷ The Bragg reflection phase plate provides an energy tunable CPX source that can rapidly reverse the helicity, but requires a highly collimated incoming beam and thus special preliminary optics. The Laue reflection phase plate, on the other hand, does not require a highly collimated incident beam or special preliminary optics to obtain a high P_c , but it cannot scan in energy or reverse the photon helicity. By working in a transmission⁵ rather than a reflection geometry, these problems encountered with the reflection-type phase plates can be overcome.

According to the dynamical diffraction theory, the σ and π wave fields propagate with different phase velocities inside the crystal, therefore a phase retardation δ can be induced between the polarization components. The degree of this birefringence is a function of the deviation of the incoming beam from the exact Bragg condition $\Delta\theta$. On the tails of the diffraction peak, this birefringence changes relatively slowly, thus relaxing the degree of collimation required in the incoming beam to obtain a well-defined polarization state. The diffracted intensity on the tails is very small, however; therefore the transmitted beam rather than the diffracted beam must be used. For Bragg diffraction, the phase difference δ between the σ and π fields for the transmitted beam is given by

$$\delta = \frac{\pi}{2} \Gamma^2 \frac{t \sin 2\theta_B}{\lambda \Delta\theta \sin \theta_B} \operatorname{Re}(F_H F_{\bar{H}}), \quad \Gamma = \frac{r_e \lambda^2}{\pi V}. \quad (1)$$

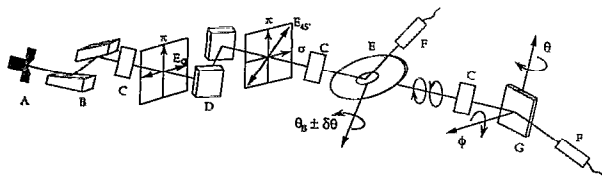


FIG. 1. Experimental arrangement at the CHESS B-2 station. A: Primary slits 0.75×3 mm; B: Asymmetric-symmetric Si (400) monochromator; C: Ionization chambers; D: Asymmetric Ge (333) linear polarizing channel-cut crystal diffracting at 45° to the horizontal; E: Bragg transmission phase plate; F: NaI detectors; G: GaAs (222)/(113) reflection diffracting horizontally for polarimetry measurements.

Here t is the crystal thickness, λ is the wavelength, F_H is the structure factor of the reflection, and r_e is the classical electron radius. The degree of circular polarization can be related to this phase difference δ and the σ and π transmitted field amplitudes, E_σ and E_π , by

$$P_c = \frac{2E_\sigma E_\pi}{|E_\sigma|^2 + |E_\pi|^2} \sin \delta. \quad (2)$$

Note that the parameter $\Delta\theta$ can be adjusted to obtain a $\pi/2$ phase shift for any particular crystal thickness and photon energy and that $\pm\Delta\theta$ results in $\pm\delta$. Therefore, for equal amounts of transmitted σ and π intensities, a single thin crystal may be used to obtain a nearly total circular polarization at any energy and the helicity can be reversed simply by moving to opposite sides of the rocking curve. Furthermore, this helicity reversal can be accomplished rapidly and frequently because it involves a movement of only a few arcsec. By operating on the tails of the reflection curve, beam divergence does not dramatically affect the polarization properties of the transmitted beam, eliminating the need for special preliminary optics. Finally, this degree of polarization is achieved with a minimal attenuation of the x-ray beam since the $\Delta\theta$ values of a few arcsec, needed to obtain a phase shift of $\pi/2$, require a Si thin crystal of only 1–2 absorption lengths.

III. EXPERIMENTAL SETUP

The measurements were performed at the CHESS B-2 bending magnet beamline. The experimental setup and optics are shown in Fig. 1. Upstream slits prior to the monochromator first defined the incoming beam to 0.75 mm×3 mm. Si (400) monochromating crystals were used for a nondispersive arrangement with the Si (400) phase plate. The first monochromator crystal was cut asymmetrically ($\alpha=25^\circ$) increasing the beam size to 4 mm×3 mm. The asymmetric cut further collimated the beam allowing for higher circular polarization rates and increased the acceptance of the monochromator providing for a higher throughput. To obtain equal amounts of σ and π polarization incident on the phase plate, the beam was diffracted by a Ge (333) channel-cut crystal with the diffracting planes oriented at 45° to the particle orbital plane. The scattering angle of this reflection is very close to 90° for 8.0 keV photons, thus this geometry rotates the natural horizontal linear polarization of the synchrotron radiation to 45°. The Ge (333) crystal was also cut asym-

metrically ($\alpha=32^\circ$) in order to obtain the maximum possible acceptance and minimize the effects of the horizontal divergence of the beam. The asymmetries of both the Si (400) monochromator and the Ge (333) linear polarizer crystals were optimized to operate in the 7.0–9.0 keV range.

The Si (400) phase plates consist of 525 μm thick, 3 in. diam wafers with a 1 in. etched center portion ($t=50, 75$, and 100 $\mu\text{m} \pm 1\%$). Rocking curve measurements were taken to confirm that the crystals were held strain free. An electrostrictive actuator (ESA) mounted on a tangential arm was used for fine rotations (<0.1 arc sec) of the phase plate, while a standard rotation stage provided for coarse angle adjustments (0.9 arc sec) and energy scanning. The polarization measurements were performed by maximizing the diffracted intensity with the ESA and then moving off the Bragg condition with the rotation stage. The position of the diffraction peak was checked periodically during polarimetry measurements.

IV. PHASE PLATE CHARACTERIZATION

A complete characterization of the polarization of the transmitted beam was made by a combination of normal Bragg diffraction and multibeam diffraction from a GaAs crystal. To obtain a direct measurement of the degree of circular polarization, a technique must be sensitive to the phase as well as to the amplitude. In a two-beam diffraction process, this phase information is lost, but in multibeam diffraction coherent interference between the wave fields of each reflection results in polarization state mixing making a direct measurement of the circular polarization possible.⁸ Therefore, an independent determination of all three Stokes–Poincaré parameters (P_1, P_2, P_3), which characterize the σ and π linear, the $\pm 45^\circ$ linear, and the left- and right-handed circular polarization, components can be made.⁹ Previous investigations of this and other types of phase plates have only indirectly measured the circular polarization rate by measuring the linear components P_1 and P_2 , then inferring the circular component P_3 from $P_3 = (1 - P_1^2 - P_2^2)^{1/2}$. This neglects possible contributions arising from unpolarized x rays, which can be on the order of 10%.⁹

The linear P_1 and P_2 polarization components were measured by diffracting from the GaAs (222) reflection with the scattering plane oriented at 0°, 90°, and $\pm 45^\circ$ with respect to the vertical. The rocking curve measurements were made at each orientation, and the integrated intensities were used to determine the normalized difference over sum ratio. While the scattering angle for this reflection is not ideal for measurements of the linear polarization, $2\theta_B=56.7^\circ$, it is still possible⁹ to obtain values for P_1 and P_2 with only slightly larger errors than measurements taken with $2\theta_B=90^\circ$. To obtain the circular component P_3 , the (222) main reflection was oriented to diffract horizontally and aligned along the ϕ rotation axis of the polarimeter. Horizontal diffraction was chosen in order to more easily remain on the peak of the main reflection while rotating ϕ . Then the crystal was scanned $\pm 0.5^\circ$ in ϕ around the (113) secondary or umweg reflection. The asymmetric profile of the secondary reflection in these scans is directly correlated to the circular component present in the beam. To extract this, the scans were fit to

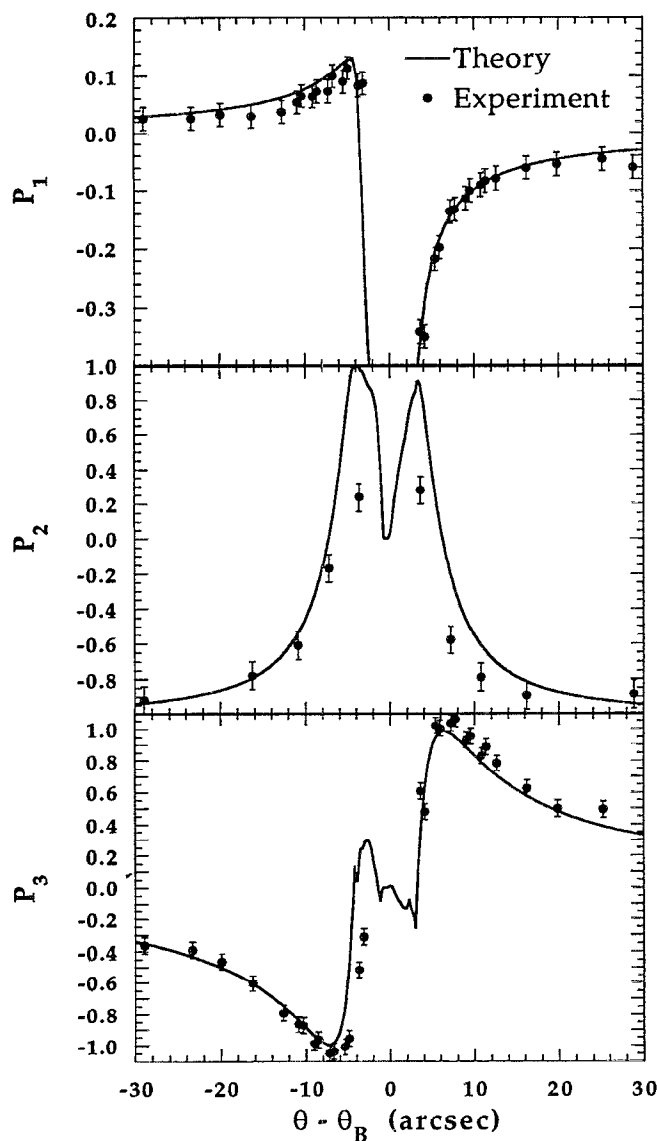


FIG. 2. Measured linear and circular polarization components along with theoretical curve for a 50 μm crystal at 8.0 keV incoming radiation $P_2 = -1.0$.

$$y = B + \frac{A_x}{x^2 + \Delta^2} + \frac{P\Delta^2}{x^2 + \Delta^2}. \quad (3)$$

Here B corresponds to the intensity of the main (222) reflection, A is the parameter describing the asymmetry of the secondary reflection, P is the peak intensity of the secondary reflection, and Δ is the HWHM of the umweg reflection. Rewriting Eq. (4) in Ref. 9 it is found that P_3 is proportional to the ratio of the asymmetry term A and the main beam intensity B plus a small correction.

V. RESULTS

The measured polarization components of the transmitted beam as a function of the off-Bragg position for a 50- μm -thick crystal and 8.0 keV photons are shown in Fig. 2 along with theoretical curves¹⁰ convoluted to account for the incoming beam divergence. There is good qualitative agreement between the data for the linear polarization components and the theoretical curves. The data for the circular polarization are all within error of the theoretical curve but tend to be slightly higher than theory giving the unphysical result of ± 1.02 for the peak P_3 polarization. This might be due to a small miscalibration of the energy which would adjust P_3 downward for equal measured asymmetry, or to a systematic error in the fits to the data overestimating the asymmetry. Even accounting for these errors, circular polarizations higher than $P_3 \geq \pm 0.95$ are seen on both sides of the diffraction peak, and the positions of the maximum polarizations line up well with theory.

In summary, we have demonstrated that a Bragg transmission phase plate provides an energy tunable high P_c CPX source, with minimal beam attenuation and easy polarization reversal. All of these qualities are unique to this CPX source, thus making this phase plate well suited to perform resonant magnetic scattering and absorption measurements.

ACKNOWLEDGMENTS

We would like to thank Al Macrander for his assistance in calculations of the theoretical polarization curves. We would also like to thank K. D. Finkelstein and Q. Shen for valuable discussions and their assistance in performing the polarimetry measurements. This work is supported by U.S. DOE-BES under contract No. W-31-109-ENG-38. Work at CHESS is supported by the National Science Foundation under Grant No. DMR-87-19764.

¹J. A. Golovchenko, B. M. Kincaid, R. A. Levesque, A. E. Meixner, and D. R. Kaplan, *Phys. Rev. Lett.* **57**, 202 (1986).

²D. Gibbs, D. R. Harshman, E. D. Isaacs, D. B. McWhan, D. Mills, and C. Vettier, *Phys. Rev. Lett.* **61**, 1241 (1988).

³G. Schütz, M. Knülle, R. Wienke, W. Wilhelm, W. Wagner, P. Kienle, and R. Frahm, *Z. Phys. B* **73**, 67 (1988).

⁴B. W. Batterman, *Phys. Rev. B* **45**, 12677 (1992).

⁵V. A. Belyakov and V. E. Dmitreinko, *Sov. Phys. Usp.* **32**, 697 (1989).

⁶K. Hirano, K. Izumi, T. Ishikawa, S. Annaka, and S. Kikuta, *Jpn. J. Appl. Phys.* **30**, L407 (1991).

⁷C. Giles, C. Malgrange, J. Goulon, F. de Bergevin, C. Vettier, E. Dartyge, A. Fontaine, C. Giorgetti, and S. Pizzini, *J. Appl. Cryst.* **27**, 232 (1994).

⁸Q. Shen and K. D. Finkelstein, *Phys. Rev. B* **45**, 5075 (1992).

⁹Q. Shen and K. D. Finkelstein, *Rev. Sci. Instrum.* **64**, 3451 (1993).

¹⁰The theoretical curves were calculated using the code described in D. W. Berreman and A. T. Macrander, *Phys. Rev. B* **37**, 6030 (1988).